TISSUE ENGINEERING: Part A
Volume 17, Numbers 23 and 24, 2011

DOI: 10.1089/ten.tea.2010.0714

Renal Tissue Engineering with Decellularized Rhesus Monkey Kidneys: Age-Related Differences

Karina H. Nakayama, B.S.,[1] Cynthia A. Batchelder, Ph.D.,[1] Chang I. Lee, Ph.D.,[1] and Alice F. Tarantal, Ph.D.[1,2]

New therapies for severely damaged kidneys are needed due to limited regenerative capacity and organ donor shortages. The goal of this study was to repopulate decellularized kidney sections *in vitro* and to determine the impact of donor age on recellularization. This was addressed by generating decellularized kidney scaffolds from fetal, juvenile, and adult rhesus monkey kidney sections using a procedure that removes cellular components while preserving the structural and functional properties of the native extracellular matrix (ECM). Kidney scaffolds were recellularized using explants from different age groups (fetal, juvenile, adult) and fetal renal cell fractions. Results showed vimentin+ cytokeratin+ calbindin+ cell infiltration and organization around the scaffold ECM. The extent of cellular repopulation was greatest with scaffolds from the youngest donors, and with seeding of mixed fetal renal aggregates that formed tubular structures within the kidney scaffolds. These findings suggest that decellularized kidney sections from different age groups can be effectively repopulated with donor cells and the age of the donor is a critical factor in repopulation efficiency.

Introduction

Twenty-six million people in the United States have chronic kidney disease with progression leading to kidney failure, a condition for which the only treatment is dialysis or whole organ transplantation.[1] Approximately 80% of individuals on the donor organ wait list are in need of a kidney. The actual number of kidney transplants still remains below 20% leaving a critical organ shortage.[2] A potential solution to ease the need for kidney donors may be through the development of functional tissue replacement using tissue engineering.

Recent advances in the field include the use of decellularized tissues as scaffolds for the re-engineering of organs including the heart,[3] trachea,[4,5] liver,[6] and lung.[7–9] Decellularized tissue matrices are useful scaffolds because they possess native extracellular matrix (ECM) and architecture that potentiate basic cell–cell and cell–ECM interactions necessary to initiate tissue formation *in vitro*. For the kidney, the spatial composition and concentration of ECM macromolecules is a component of well-orchestrated interactions that ensures normal nephrogenesis.[10] Age-dependent generation of functional renal structures has previously been demonstrated by Woolf *et al.*[11] where it was shown that new nephrons were generated from metanephroi transplanted into neonatal, but not adult, mice. Our studies have also previously demonstrated effective procedures for decellularizing kidney scaffolds and shown the capacity of these scaffolds to support cell attachment and migration, and suggested that success was dependent on donor age.[12]

The goal of the current study was to more fully address age-related differences using kidney sections from different age groups and prove our hypothesis that decellularized kidney scaffolds from different age groups can be repopulated with donor cells in an age-dependent manner. These studies provide new information on regenerative strategies and the impact of age on repopulation efficiency.

Materials and Methods

Tissue collection

All animal protocols were approved before implementation by the Institutional Animal Care and Use Committee at the University of California, Davis, and all procedures conformed to the requirements of the Animal Welfare Act. Activities related to animal care were performed in accordance with standard operating procedures at the California National Primate Research Center (CNPRC). Tissue harvests were performed using established methods and protocols.[13] Kidney transverse sections were collected from fetal (mid to late third

[1]Center of Excellence in Translational Human Stem Cell Research, California National Primate Research Center, [2]Departments of Pediatrics and Cell Biology and Human Anatomy, University of California, Davis, California.

trimester) ($n=10$), juvenile (3 months to 1.5 years postnatal age) ($n=7$), and adult (5–13 years of age) ($n=4$) rhesus monkeys (*Macaca mulatta*) for decellularized scaffolds as previously described.[12] Sections were also collected from third trimester fetuses ($n=8$), juveniles (3 months to 1.5 years postnatal age) ($n=3$), and adults ($n=2$) for explants and fetal kidney cell fractions (total $n=34$) (Table 1). The number of animals selected for use in this study was determined to be sufficient based on our prior studies[14] where statistical significance was shown with a similar number of animals ($n=3$) per age group. All tissues were placed in Dulbecco's modified Eagle's medium (DMEM) (Gibco, Invitrogen) upon collection with processing conducted at the time of tissue harvest.

Decellularization

Kidney decellularization was performed using established protocols.[13] Briefly, kidney transverse sections were washed twice with phosphate-buffered saline (PBS) (Gibco, Invitrogen) followed by a decellularization solution of 1% (v/v) sodium dodecyl sulfate (Invitrogen) diluted in distilled water at 4°C. The solution was changed 8 h after initial tissue harvest and then every 48 h until the tissue was transparent (7–10 days). Decellularized kidney scaffolds were gently washed with PBS and either fixed in 10% phosphate buffered formalin (Thermo Fisher Scientific) and embedded in paraffin, or stored in 10% (v/v) penicillin/streptomycin (Gibco, Invitrogen) in PBS at 4°C until use. Explants or cell fractions and scaffolds were paired with different donors (see Table 1).

Recellularization with layered explant/scaffold

Before recellularization, stored scaffolds were soaked overnight in sterile filtered (0.22 μm pore size; Millipore) 70% (v/v) ethanol in super-Q water and rehydrated in 10% penicillin/streptomycin in PBS for 48 h. Fetal, juvenile, or

Table 1. Study Overview

Approach	*Cell donor*	*Scaffold donor*		
1. Explant/scaffold	Fetus A	Fetus #1	Juvenile #1	Adult #1
	Fetus B	Fetus #1	Juvenile #1	Adult #1
	Fetus C	Fetus #1	Juvenile #1	Adult #1
	Juvenile A	Fetus #2	Juvenile #2	Adult #2
	Juvenile B	Fetus #3	Juvenile #3	Adult #1
	Juvenile C	Fetus #3	Juvenile #3	Adult #1
	Adult A	Fetus #4	Juvenile #1	Adult #3
	Adult B	Fetus #4	Juvenile #1	Adult #3
	Adult C	Fetus #5	Juvenile #5	Adult #1
2. Fetal renal Fractions 1 and 2				
Intact Fraction 1	Fetus D	Fetus #6	Juvenile #1	—
	Fetus E	Fetus #7	Juvenile #3	—
	Fetus F	Fetus #8	Juvenile #4	—
Dissociated Fraction 1	Fetus D	Fetus #6	Juvenile #1	—
	Fetus E	Fetus #7	Juvenile #3	—
	Fetus F	Fetus #8	Juvenile #4	—
Intact Fraction 2	Fetus D	Fetus #6	Juvenile #1	—
	Fetus E	Fetus #7	Juvenile #3	—
	Fetus F	Fetus #8	Juvenile #4	—
Dissociated Fraction 2	Fetus D	Fetus #6	Juvenile #1	—
	Fetus E	Fetus #7	Juvenile #3	—
	Fetus F	Fetus #8	Juvenile #4	—
3. Fetal renal Fraction 2 with different media				
Intact (medium only)	Fetus G	Fetus #5	Juvenile #5	Adult #4
	Fetus H	Fetus #9	Juvenile #6	Adult #4
	Fetus I	Fetus #10	Juvenile #7	Adult #4
Dissociated (medium only)	Fetus G	Fetus #5	Juvenile #5	Adult #4
	Fetus H	Fetus #9	Juvenile #6	Adult #4
	Fetus I	Fetus #10	Juvenile #7	Adult #4
Intact (medium + FGF)	Fetus G	Fetus #5	Juvenile #5	Adult #4
	Fetus H	Fetus #9	Juvenile #6	Adult #4
	Fetus I	Fetus #10	Juvenile #7	Adult #4
Dissociated (medium + FGF)	Fetus G	Fetus #5	Juvenile #5	Adult #4
	Fetus H	Fetus #9	Juvenile #6	Adult #4
	Fetus I	Fetus #10	Juvenile #7	Adult #4
Intact (EGM-2)	Fetus G	Fetus #5	Juvenile #5	Adult #4
	Fetus H	Fetus #9	Juvenile #6	Adult #4
	Fetus I	Fetus #10	Juvenile #7	Adult #4
Dissociated (EGM-2)	Fetus G	Fetus #5	Juvenile #5	Adult #4
	Fetus H	Fetus #9	Juvenile #6	Adult #4
	Fetus I	Fetus #10	Juvenile #7	Adult #4

FGF, fibroblast growth factor (4 ng/mL) added to culture medium; EGM-2, endothelial cell growth medium-2.

adult kidney explants ($n=3$ per age group; total $n=9$) were layered on an age-matched (3 per age group) or non-age-matched (3 per age group) decellularized kidney scaffolds (see Table 1) and cultured in explant medium (500 mL DMEM/F12, Invitrogen; 25 ng/mL prostaglandin E, Sigma; 1% insulin/transferrin/selenium, Sigma; 10% fetal bovine serum [FBS], Gibco; 1% penicillin/streptomycin) for 7 days. Unless otherwise stated, all recellularization cultures were performed in transwell inserts (1 cm diameter). After 7 days in culture, layered explants were fixed in 10% formalin, embedded in paraffin, and stained with hemotoxylin and eosin (H&E) and immunohistochemistry (IHC) was performed as described below. Photomicrographs were obtained with an Olympus production microscope.

Recellularization with fetal renal fractions

In a preliminary study a comparison of second (early and mid) and third (early, mid, and late) trimester fetal renal cell fractions (Fraction 2, *intact* or *dissociated*; see below) was conducted ($n=5$) and showed no differences in the extent of cell infiltration and infiltration distance, location of cells within the scaffold, or cellular phenotype when compared. Based on these findings, the study was performed with third trimester fetal kidney donor cells as noted above. Isolation of renal structures from third trimester fetuses was adapted from Kreisberg and Karnovsky.[15] Fresh kidney sections were minced in 0.1% collagenase and filtered through 160-μm nylon mesh (Millipore) followed by a 40-μm mesh cell strainer (Millipore) (Fig. 1). Fraction 1 consisted of glomeruli that were collected by inverting the 40-μm filter and washing with PBS. Fraction 2 consisted of a heterogeneous mixture of renal tissue aggregates (tubules, interstitial tissue, some glomeruli) and was collected by scraping the top of the 160-μm filter. Renal structures from each fraction were centrifuged at 800 rpm for 5 min to create a loose pellet that was then resuspended in explant culture medium. Fractions 1 and 2 were seeded onto previously decellularized fetal ($n=3$) or juvenile ($n=3$) kidney scaffolds and chamber slides

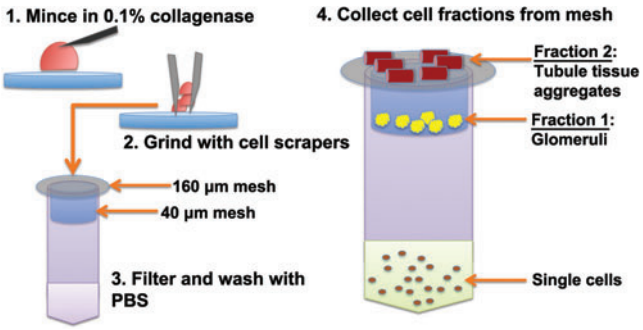

FIG. 1. Methods used for separation of renal structures. *Intact* Fraction 1 (glomeruli) was collected by inverting the 40-μm filter and washing with medium. *Intact* Fraction 2 (mixed tubular aggregates) was obtained by gently scraping the top of the 160-μm filter with cell scrapers followed by several washes with medium. *Dissociated* Fraction 1 and Fraction 2 were obtained by trypsinization of cells that grew from the culture of *intact* Fraction 1 and Fraction 2 followed by passage of cells through a 40-μm filter. Color images available online at www.liebertonline.com/tea

(Thermo Scientific) in two different conditions: either as intact fresh renal structures (Fraction 1 or 2, *intact*) or as dissociated single cells (Fraction 1 or 2, *dissociated*). Fraction 1 *intact* represented whole glomeruli, whereas Fraction 2 *intact* represented mixed tubular aggregates. Fraction 1 or 2 *dissociated* represented cells that migrated onto tissue culture plastic over 4–5 days from the Fraction 1 or 2 *intact* structures. These cells were collected by trypsinization followed by passage through a 40-μm filter. The renal structures obtained from one fresh kidney transverse section were used to seed two scaffolds. Approximately 500,000 dissociated cells were seeded per scaffold. Cells on scaffolds and chamber slides were analyzed with IHC or immunocytochemistry (ICC), respectively. ICC was performed on the *intact* fraction after a few days in culture to obtain three-dimensional structures. ICC on the *dissociated* fraction was accomplished after 1 day in culture of the passaged single cells that had grown from intact structures on tissue culture plates as noted above. Only fetal and juvenile scaffolds were used in these experiments to initially test repopulation efficiency using fetal cell fractions. Thus, these experiments examined two cell fractions (Fraction 1 and 2), each in two different cell states (*intact* vs. *dissociated*), and on two different aged scaffolds (fetal or juvenile).

Recellularization with fetal renal fractions ± fibroblast growth factor or endothelial cell growth medium-2

These studies examined only Fraction 2 cells (*intact* vs. *dissociated*) and with three different aged scaffolds (fetal, juvenile, and adult), each with three different culture media conditions. Fraction 2 *intact* or *dissociated* were seeded onto fetal, juvenile, or adult scaffolds ($n=3$ per scaffold age group) and cultured for 7 days under the following culture conditions: (1) explant medium only, (2) explant medium + 4 ng/mL human fibroblast growth factor (FGF), or (3) endothelial cell growth medium-2 (EGM-2) (Lonza) with full supplements (10% FBS, 0.4% FGF, 0.1% vascular endothelial growth factor, 0.1% R^3-insulin-like growth factor-I, 0.1% human epidermal growth factor, 0.04% hydrocortisone, 0.1% ascorbic acid, 0.1% heparin, 0.1% GA-1000 [Gentamicin, Amphotericin-B]). All seeded scaffolds were fixed in formalin and embedded in paraffin for analysis.

Cell infiltration

The extent of repopulation of the kidney scaffolds by the layered explant or renal fractions was quantified by measuring the distance of tubular structures from the scaffold/explant border or the scaffold surface. The distance of each structure as well as the total number of tubules was averaged for each group (see below).

Morphology

All sections were stained with H&E to assess morphology. ICC and IHC were performed on chamber slides and on paraffin-embedded sections (5–6 μm), respectively, for cytoskeletal and renal-specific proteins using established protocols.[13,16] Briefly, chamber slides were washed in PBS for 5 min before fixing in cold methanol for 10 min at ≤ −20°C. Slides were blocked with 2% goat serum (Sigma-Aldrich) in blocking buffer (1% BSA in PBS) for 20 min at room

temperature. After washing twice with PBS, slides were incubated with primary antibody diluted in blocking buffer overnight in a humidified chamber at 4°C. Primary antibodies used were paired box gene 2 (Pax2, Polyclonal; Invitrogen) diluted 1:100, Wilms tumor 1 (WT1, clone 6F-H2; Invitrogen) diluted 1:100, wide spectrum cytokeratin (polyclonal; Abcam) diluted 1:50, and vimentin (clone V6389; Sigma) diluted 1:100, smooth muscle actin (SMA, clone ASM-1; Millipore) diluted 1:100, calbindin (polyclonal; Millipore) diluted 1:100, and cluster of differentiation molecule 31 (CD31, clone JC/70A; Thermo Scientific) diluted 1:100. Mouse immunoglobulin G1 (IgG1) (Dako), mouse IgG2a (Dako), and rabbit IgG (Invitrogen) isotype controls were also used. Slides were washed twice for 5 min with PBS and then incubated with secondary antibody dilutions for 1 h in the dark at room temperature. Secondary antibodies used were Alexa Fluor 488 goat anti-mouse (Invitrogen) and Alexa Fluor 594 goat anti-rabbit (Invitrogen) diluted 1:200 in blocking buffer. Slides were washed twice with PBS before mounting with 1 drop of ProLong® Gold antifade reagent with 4,6′-diamidino-2-phenylindole (DAPI) (Invitrogen) and then a coverslip was placed. Slides were stored at ≤−20°C until photomicrographs were taken with an Olympus production microscope.

For paraffin sections, the sections were rehydrated in xylene followed by graded concentrations of ethanol.[13,17] Slides were washed in PBS before heat-mediated antigen retrieval in citrate buffer (pH 6; Invitrogen) was performed. After cooling, decreasing concentrations of warm citrate buffer in PBS was applied followed by incubation with Background Sniper (BioCare Medical), which was added to each slide for 15 min. Slides were washed twice with PBS followed by incubation for 1 h with blocking buffer (1% BSA, 0.1% fish skin gelatin, 0.1% Triton X, 0.05% tween-20) with 2% goat serum (Sigma-Aldrich). After two washes with PBS, primary antibody diluted in primary antibody buffer (1% BSA, 0.1% fish skin gel) was incubated with slides overnight in a humidified chamber at 4°C. Primary antibodies used were HLA-DR (Invitrogen), a major histocompatability complex (MHC) class II cell surface receptor. Human leukocyte antigen (HLA)-DR was diluted 1:50, Pax2 diluted 1:100, WT1 diluted 1:100, wide spectrum cytokeratin diluted 1:50, and vimentin diluted 1:100. Mouse IgG1 and rabbit IgG isotype controls were included as noted. Slides were washed with PBS for 5 min and incubated with secondary antibody for 1 h in the dark at room temperature. Secondary antibodies used were Alexa Fluor 488 goat anti-mouse and Alexa Fluor 594 goat anti-rabbit diluted 1:200 in fluorescence antibody diluent (BioCare Medical). After washing twice with PBS, slides were mounted with ProLong Gold antifade reagent with DAPI (Invitrogen) and a coverslip placed.

Quantitative real-time polymerase chain reaction

Quantitative real-time polymerase chain reaction (qRT-PCR) was used to measure the expression of renal markers including aquaporin-2 (water channel, proximal tubules), CD31 (glomerular endothelium), nestin (podocytes), Pax2 (induced metanephric mesenchyme), synaptopodin (podocytes), vimentin (mesenchyme), WT1 (induced metanephric mesenchyme, renal vesicle, early podocytes), and the housekeeping gene elongation factor 1-alpha (EF1-α)[12,16] (Table 2). Total RNA was extracted from cells preserved in RLT buffer at ≤−20°C using the RNeasy kit (RNeasy® Plus Mini Kit; Qiagen) following the manufacturer's instructions. cDNA was synthesized using random primers (Ambion) and the Sensiscript Reverse Transcriptase kit (Qiagen). Primers were designed to span an exon junction. qRT-PCR was carried out in 96-well optical plates using the 7900® ABI Sequence Detection System (Applied Biosystems) and the QuantiTect™ SYBR® Green PCR Kit (Qiagen) according to the manufacturer's protocols. PCR was run in duplicate in separate wells and contained 1×SYBR Green master mix and 300 nM of forward and reverse primers in a 25 μL reaction volume. The PCR protocol consisted of one cycle of 2 min at 50°C, 15 min at 95°C, followed by 40 cycles at 15 s at 95°C, and 60 s at 60°C. RNA expression was quantified according to the Comparative C_T method described in User Bulletin #2 (Applied Biosystems; updated 2001) relative to the housekeeping gene EF1-α.[12] Positive and negative controls (water)

Table 2. Primer Sequences

Gene (marker)	*Primer*	*Sequence*
Aquaporin-2	Forward primer	5′-CCGCTCTGCTCCATGAGATC-3′
	Reverse primer	5′-TGCTGTTGCTGAGAGCATTGA-3′
CD31	Forward primer	5′-GAGTATTACTGCACAGCCTTCAACAG-3′
	Reverse primer	5′-AACCACTGCAATAAGTCCTTTCTTC-3′
Nestin	Forward primer	5′-TGGCAAGAGGCCGGTACA-3′
	Reverse primer	5′-CCGTATTTGTCCTTCACCTTCCT-3′
Pax2	Forward primer	5′-GCTTTGGATCGGGTCTTTGA-3′
	Reverse primer	5′-CTCGTTCCCCTGTTCTGATTTG-3′
Synaptopodin	Forward primer	5′-CAGATTGGGCCAGAGCACTAG-3′
	Reverse primer	5′-TTGGACGCCACGGGAAT-3′
Vimentin	Forward primer	5′-TGCCCTTAAAGGAACCAATGAGT-3′
	Reverse primer	5′-TAGCAGCTTCAACGGCAAAGT-3′
WT1	Forward primer	5′-CTTCAGAGGCATTCAGGATGTG-3′
	Reverse primer	5′-TCTCAGATGCCGACCGTACA-3′
EF1-α	Forward primer	5′-GACCCACCAATGGAAGCAG-3′
	Reverse primer	5′-TGTGGCAATCCAATACAGGG-3′

WT1, Wilm's tumor 1; Pax2, paired box 2; EF1-α, housekeeping gene elongation factor 1-alpha.

were included in each run. The results were calculated as relative transcription or the *n*-fold difference relative to a calibrator cDNA. Primary fetal renal cortical cells from a similar age group that were previously collected and cryopreserved were used for comparison to intact Fraction 1 and Fraction 2 gene expression. Intact Fraction 2 was used as a calibrator for comparison of *intact* versus *dissociated* Fraction 2 gene expression. All Fraction 1 and Fraction 2 specimens were cryopreserved on the day of collection.

Data analysis

All data are shown as mean with the standard error of the mean. Statistical analysis was performed using a two tailed Student's *t*-test and $p < 0.05$ were considered statistically significant.

Results

Age-related differences

We previously reported methods for decellularization of rhesus monkey kidney transverse sections to produce kidney scaffolds with intact ECM proteins and complete removal of cells including the absence of the MHC class II cell surface receptor, HLA-DR. Two different strategies for recellularization of the kidney scaffold were investigated in these studies. The first strategy utilized fresh kidney explants from different age groups (fetal, juvenile, adult) as the cell source. Explants were layered on either age-matched or non-age-matched decellularized kidney scaffolds (Table 1). The extent of cell infiltration from the explant into the scaffold was assessed by measuring the distance from the explant/scaffold border to the tubular structures that repopulated the scaffold (Fig. 2A). Fetal explants demonstrated a tubular population that infiltrated the scaffolds of all age groups; however, juvenile and adult explants did not repopulate the scaffolds of different age groups in a comparable manner. Infiltration distances of tubules for age-matched fetal explants on fetal scaffolds were significantly greater than juvenile explants on juvenile or adult scaffolds, or adult explants on scaffolds of all age groups. Tubular infiltration from the explants into the scaffolds was most extensive with fetal and juvenile scaffolds when compared to adult scaffolds (Fig. 2B). These studies suggest that both the age of the donor cell source and the age of the donor scaffold play a role in effective cellular repopulation of decellularized kidney scaffolds.

Cells that infiltrated the scaffold were found to be of two phenotypes: individual cells that were vimentin+ Pax2+ (mesenchymal) and clustered cells that were vimentin+ Pax2+ cytokeratin+ (epithelial) (Fig. 3). The infiltration of tubular cells from fetal explants into fetal or juvenile scaffolds resulted in small clusters of tubular structures within the scaffolds that were positive for vimentin, Pax2, and cytokeratin. These structures showed similar polarization of epithelial and mesenchymal markers when compared to the explant.

Characterization of fetal renal fractions

The second strategy for recellularization of the scaffolds was seeding of *intact* fetal Fraction 1 or Fraction 2 renal structures as well as *dissociated* Fraction 1 and 2 cells onto fetal or juvenile scaffolds. These different cell populations were characterized by ICC for vimentin, cytokeratin, Pax2, and WT1 (Fig. 4). Expression of WT1 was maintained in the glomerular population in both *intact* and *dissociated* Fraction 1. *Intact* Fraction 2 indicated cells were positive for either cytokeratin or vimentin; however, the *dissociated* Fraction 2 cells contained a population that strongly coexpressed vimentin and cytokeratin, possibly suggesting mesenchymal-epithelial transformation. In addition, Pax2 expression was diminished in *dissociated* Fraction 2 when compared to *intact* Fraction 2. These data suggest that the dissociation process, which involves outgrowth of cells onto tissue culture plastic followed by a single passage and time in culture, may have altered the cell phenotype when compared to *intact* fractions.

Analysis of relative gene expression by qRT-PCR showed that *intact* Fraction 1 expressed markers associated with the glomerular tuft (CD31) with a 3-fold increase, WT1 with a 6-fold increase, and synaptopodin with a 20-fold increase compared to primary fetal renal cortical cells and confirmed their glomerular origin. *Intact* Fraction 2 demonstrated expression of nestin typically shown on tubulointerstitial cells during kidney development as well as aquaporin-2, a marker of proximal tubules[18] confirming the presence of tubular cells. *Dissociated* Fraction 2 demonstrated higher levels of expression of vimentin and lower expression of early renal markers and aquaporin-2 compared to *intact* Fraction 2, supporting the ICC results noted above and suggesting that intact structures likely provide a cell source that retains the desired renal phenotype for recellularization.

Recellularization with fetal renal fractions: infiltration distance

Comparison of *intact* versus *dissociated* Fraction 1 and Fraction 2 fetal renal cells showed a similar outcome for all

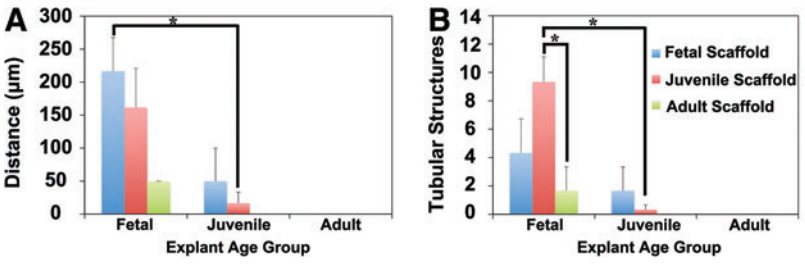

FIG. 2. Age-related differences in tubular infiltration. Fetal, juvenile, or adult explants were layered on fetal, juvenile, or adult scaffolds. The extent of cell infiltration from the explant into the scaffold was determined by the average distance from the explant/scaffold border. **(A)** The distance for infiltration is shown as mean infiltration distance with the standard error of the mean (SEM). The greatest infiltration distance was observed with fetal explants on fetal scaffolds. *$p < 0.05$. **(B)** The number of tubules for each explant/scaffold age group is shown as mean tubular number with SEM. The greatest number of tubules was observed with fetal explants on juvenile scaffolds. *$p < 0.05$. Color images available online at www.liebertonline.com/tea

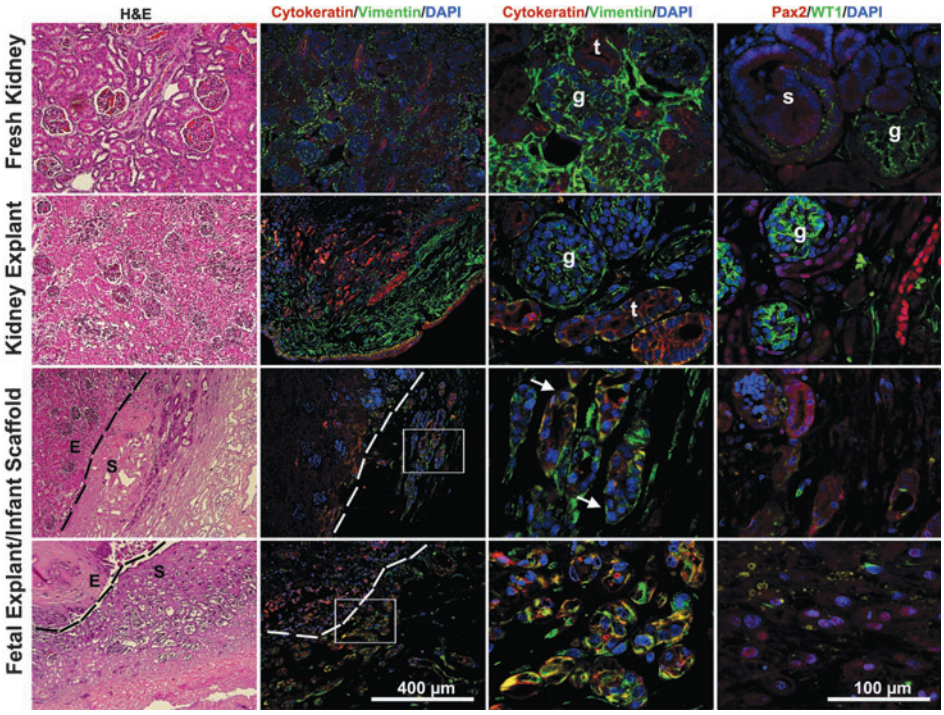

FIG. 3. Hemotoxylin and eosin (H&E) and immunohistochemical staining of fetal explants layered on juvenile scaffolds. Native kidney as well as explant-cultured kidneys are included for reference. Glomerulus (g), tubules (t), S-shaped body (s). The greatest tubule infiltration numbers were observed with fetal explants on juvenile scaffolds; therefore, staining of this representative example is shown. Dotted line in the H&E image denotes the boundary between the explant (E) and scaffold (S). The white box highlights the region magnified in the 40× image. Cell clusters in the scaffolds were positive for vimentin, cytokeratin, and paired box 2 (Pax2). Formation of tubular structures is noted (arrows).

intact and *dissociated* combinations. Although infiltration distances were similar when using *intact* fractions, seeding of *intact* Fraction 2 onto juvenile scaffolds yielded the greatest infiltration distance compared to all of the other scaffold and cell combinations. Comparison of *intact* Fraction 2 to all *dissociated* Fraction 1 and Fraction 2 combinations showed the tubular repopulation distance was significantly greater ($p < 0.05$) with *intact* Fraction 2 structures compared to *dissociated* fractions, where no evidence of tubular infiltration was observed (Fig. 5A). However, comparison of *intact* Fraction 1 to *dissociated* Fraction 1 showed no significant differences in tubular repopulation distance or content regardless of whether intact or dissociated fractions were used. Therefore, when the cell fraction was constant (1 or 2) and the condition varied (*intact* vs. *dissociated*) differences in tubular repopulation were observed for Fraction 2 but not Fraction 1. Taken together, these data suggest that the cell fraction as well as the condition of the cells impacted the degree of cellular repopulation.

Recellularization with fetal renal fractions: tubule number and phenotype

Assessment of total tubule number showed that seeding of *intact* Fraction 2 onto juvenile scaffolds produced significantly more tubular structures within the scaffold compared to all other intact or dissociated fraction/scaffold combinations, and with a phenotype similar to the layered explant

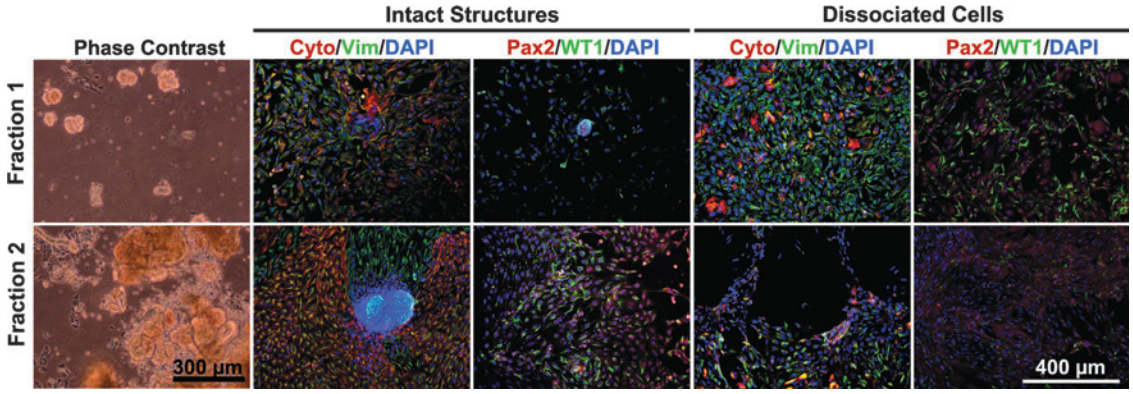

FIG. 4. Characterization of fetal renal fractions. Phase-contrast and immunocytochemistry for vimentin, cytokeratin, Pax2, and Wilms tumor 1 (WT1) for renal fractions (10×). Fraction 1 represents a glomerular population and Fraction 2 is a mixed population collected from tubular tissue aggregates. *Intact* Fraction 1 was positive for vimentin and cytokeratin. *Intact* Fraction 2 was initially positive for vimentin, cytokeratin, and Pax2. Differences between the *intact* and *dissociated* populations are shown by a decrease in Pax2 expression with *dissociated* Fraction 2, but no major differences between *intact* and *dissociated* Fraction 1 populations were noted.

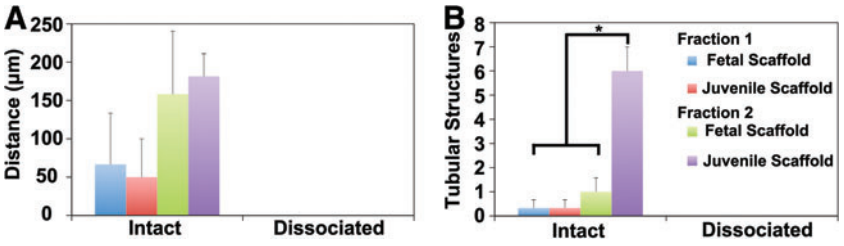

FIG. 5. Recellularization with renal Fraction 1 or Fraction 2. **(A)** The extent of tubular repopulation of the scaffold was determined by the average distance from the scaffold surface. Distances for each fraction/scaffold age group is shown as mean infiltration distance with SEM. The greatest total tubular infiltration distances were noted with *intact* Fraction 2 seeded on juvenile scaffolds. **(B)** Number of tubules in each fraction/scaffold age group reported as mean tubule number with SEM. The greatest total tubule number was shown with *intact* Fraction 2 seeded on juvenile scaffolds. $*p < 0.05$. Color images available online at www.liebertonline.com/tea

model (Fig. 5B). These tubular structures were located throughout the depth of the scaffold (400–500 μm from scaffold surface) and were positive for vimentin, cytokeratin, Pax2, and calbindin, a marker of collecting ducts (Fig. 6). A longitudinal view of the tubular structures revealed a lumen and branching. Some of the structures lacked fully developed lumens but demonstrated initial polarization of epithelial and mesenchymal markers in a semiorganized structure. Markers of cells of possible endothelial or glomerular origin, including CD31 and SMA, respectively, were not present in tubular structures. A few rare cells clustered at the scaffold surface expressed SMA. No tubular structures were found in scaffolds seeded with *dissociated* Fraction 1 or 2, suggesting that *intact* fractions may be required for infiltration and to produce extensive tubular repopulation.

Recellularization with renal fractions ± FGF or EGM-2

To further investigate the efficiency for scaffold repopulation, and to focus on the tubular cell populations, only Fraction 2 renal cells were seeded onto fetal, juvenile, or adult scaffolds and cultured in FGF-enriched explant medium or EGM-2 (Fig. 7). Tubular infiltration and maturation when using *intact* Fraction 2 was enhanced with FGF-enriched medium, whereas scaffold recellularization with *dissociated* Fraction 2 was enhanced when using EGM-2 and contained cells throughout the depth of the scaffold. All repopulated constructs had Pax2+ cell populations with two distinct phenotypes. One population was represented by individual cells dispersed throughout the scaffold, which occupied small open spaces in the ECM, and were vimentin+. The second population represented individual cells frequently found in cell clusters that displayed coexpression of vimentin and cytokeratin as well as strong expression of calbindin, but not CD31. Regardless of age, when scaffolds were seeded with *dissociated* Fraction 2, the clusters were multilayered and assembled at the scaffold surface, but they were not organized into distinct tubular structures and contained a small number of SMA+ cells. In contrast, when scaffolds were seeded with *intact* Fraction 2, the cell clusters resembled tubules with distinct lumens and polarization of apical epithelial surfaces and transitional epithelium/mesenchyme on the basolateral surface. These tubules were calbindin+ and showed no evidence of either CD31 or SMA. These structures were found several hundred microns from the scaffold surface. The tubules found within these scaffolds possessed lumens and distinct epithelial/mesenchymal polarization suggesting the addition of cytokines enhanced tubule morphology.

Discussion

A devastating 6% mortality has been reported for patients who die while waiting for a kidney to become available for transplant.[2] Donor shortages might be overcome with the development and refinement of engineered organs. While some engineered tissues using decellularized matrices such as bladder[19] and the upper airway[4] are under study in human clinical trials, the kidney remains an organ that has proven difficult to regenerate with 28 different cell types and complex metabolic functions.[20] Decellularized renal matrices have been reported to support cell attachment,[21] but the formation of renal structures with functional capacity has yet to be shown. The goal of these studies was to study engineered renal tissue from decellularized matrices that possess basic renal ECM in a clinically relevant rhesus monkey model, and to determine whether age has an impact on cellular repopulation. While kidney diseases affect all individuals at all ages it is possible that different approaches may be needed depending on the disease and the age group.[22]

We previously reported effective methods to decellularize kidney scaffolds that are free of MHC Class II antigens.[13] In the studies described herein, we initially recellularized fetal, juvenile, and adult kidney scaffolds using kidney explant culture and showed that the younger donor explants layered on scaffolds derived from all of the age groups demonstrated the most extensive cell infiltration and repopulation. Layered fetal explants were frequently found with large numbers of single cells and unorganized cell clusters of an epithelial and mesenchymal phenotype throughout the scaffold. The distance of tubular branching from the explant was measured to assess scaffold repopulation. The initial use of explants as the cell source maximized scaffold to cell contact surface area and provided a diverse mixture of native kidney cell populations. As the kidney matures (fetus to postnatal), the ECM remodels creating a different ECM landscape. Zhang *et al.*[23] described enhanced proliferation and differentiation of tissue-matched cell types with their tissue specific ECM, which underscored the sensitivity of cells to the unique ECM composition with which they were presented. Tottey *et al.*[24] demonstrated differences in mechanical and biological properties, including growth factor concentration and mitogenic cell response, of decellularized small intestinal submucosa-ECM from different aged pigs. Complex changes in the ECM that occur with age are likely responsible for differing degrees of repopulation of scaffolds with less extensive repopulation of adult scaffolds. This suggests that a more defined cytokine-enhanced culture system may be required for more mature age groups. We have previously

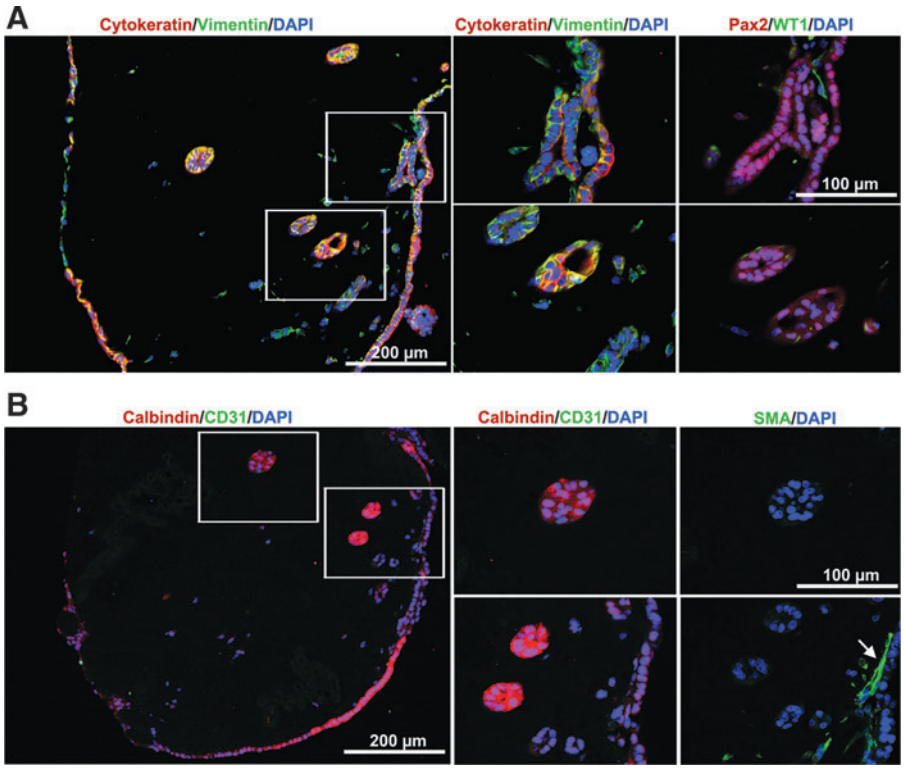

FIG. 6. H&E and immunohistochemistry (IHC) of recellularized juvenile scaffolds. IHC for vimentin, cytokeratin, Pax2, and WT1 **(A)** and calbindin, CD31, and smooth muscle actin (SMA) **(B)** on juvenile scaffold with *intact* Fraction 2. White boxes highlight the regions magnified in 40× images. When seeded with *intact* Fraction 2, tubular structures were observed throughout fetal and juvenile scaffolds (juvenile shown), and some appeared to undergo branching morphogenesis. Tubular structures were Pax2+ calbindin+ with polarized expression of cytokeratin on the luminal surface and vimentin on the basolateral surface. Rare SMA+ cells were noted near the scaffold surface (arrow).

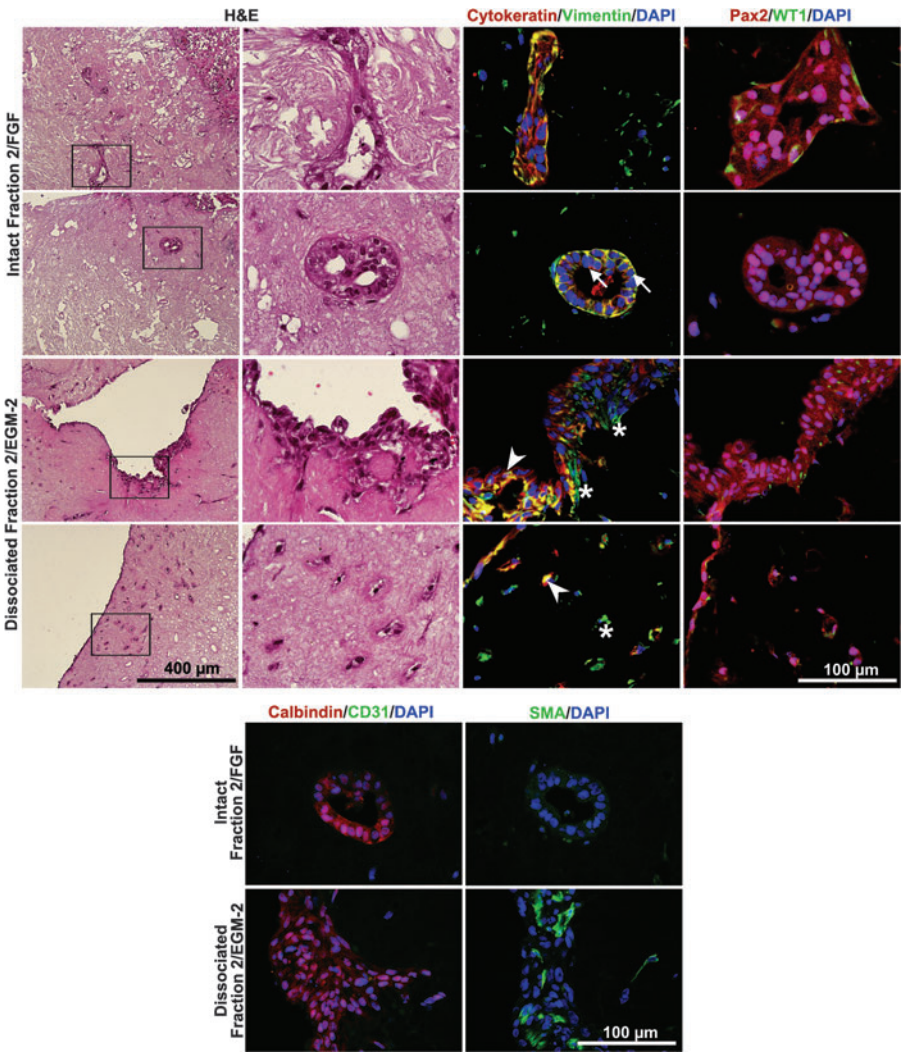

FIG. 7. Scaffolds recellularized with *intact* or *dissociated* Fraction 2 tubular aggregates cultured in fibroblast growth factor (FGF) or endothelial cell growth medium-2 (EGM-2). IHC for vimentin/cytokeratin, Pax2/WT1, calbindin/CD31, and SMA. Scaffolds repopulated with *intact* Fraction 2 with FGF contained tubular structures that were Pax2+ cytokeratin+ (lumen), and double positive for cytokeratin and vimentin on the basolateral surface (arrows). Tubular structures were calbindin+ and did not express CD31 or SMA. *Dissociated* Fraction 2 with EGM-2 demonstrated repopulation of scaffolds with cells throughout the depth of the scaffold. Two cell populations are shown: single vimentin+ cells at a distance from the scaffold surface (asterisks), and vimentin+ cytokeratin+ cells close to the surface which were occasionally found in clusters (arrowheads). The cell cluster populations were calbindin+ and contained a few SMA+ cells.

demonstrated lifespan differences in a variety of stem and progenitor cell populations, including mesenchymal,[25,26] hematopoietic,[27] and endothelial progenitor[28] cells, highlighting the importance of consideration of age in regenerative medicine strategies. Other studies have indicated that transplantation of fetal kidney cells from earlier gestational age kidneys resulted in enhanced structural formation when compared to cells obtained from later gestation kidneys.[29,30] The impact of age has been extended in the current study to span fetuses, juveniles, and adults and has demonstrated age-dependent recellularization of kidney sections, suggesting that critical differences in cell and ECM composition are important factors in renal tissue engineering and must be taken into consideration when addressing the age of the recipient.

To better understand the mechanism of recellularization, *intact* or *dissociated* renal fractions were seeded onto fetal or juvenile scaffolds. Only when scaffolds were seeded with *intact* Fraction 2 were tubular structures found to extensively repopulate the scaffold based on number of tubules and infiltration distance. All other fraction/scaffold combinations yielded significantly fewer or no tubules. These findings suggest that *intact* Fraction 2 was responsible for tubular repopulation of the scaffolds most likely by the infiltration of existing tubules rather than the generation of new tubules from single dissociated cells. Several recent studies have focused on decellularized matrices in other organ systems[4,9] and utilized dissociated cell populations; however, a different cell-based approach may be needed to re-engineer the kidney. Although *dissociated* Fraction 1 and 2 were shown to form kidney structures in a collagen matrix in other studies,[31] the dissociated cells were filtered through a strainer with pore sizes that were of a sufficient size to allow small glomeruli or tubules to readily pass through and thereby contribute to the observed glomerular structures. In addition, these fractions were seeded at a much higher density than in the study described herein. It is possible that greater seeding density may be required to increase cell–cell and cell–ECM contact, although there is currently no data to support this assumption. Although a renal tubular stem cell has not been identified, the possibility of an epithelial stem/progenitor cell within the tubules has been suggested by Humphreys *et al.*[32] These investigators showed that there were no cells of nontubular origin present in renal tubules before or after injury, suggesting that tubular repair may be performed by cells of tubular origin and not from cell populations located at other anatomical sites within the kidney. A recent publication by this group has also noted that injured epithelial cells of the proximal tubule repopulate the kidney epithelium by self-duplication of surviving epithelia, in the absence of any specialized progenitor population.[33] In the current study, an epithelial tubule population as described by Humphreys *et al.*[32,33] may be responsible for infiltration into the scaffold and could explain why fewer numbers of tubular structures were observed with Fraction 1 repopulation, which would not have contained many tubular cells. Although the kidney has demonstrated some capacity for repair in response to injury, a renal stem cell has yet to be found which underscores the necessity to explore multiple cell types for recellularization.[34]

These findings also suggest that a mixture of renal cells using intact fractions may be required for more complete tubular infiltration. The mechanical separation process used to obtain glomeruli in Fraction 1 removes Bowman's capsule, which has been shown to include a CD24+ CD133+ renal progenitor population that is present throughout kidney development and contributes to podocytes and tubular epithelium.[35,36] Alternative methods that preserve Bowman's capsule may yield enhanced scaffold recellularization by retaining this cell population. Fraction 2 contained a heterogeneous mixture of intact tubular aggregates, including occasional glomeruli with Bowman's capsule, which may have contributed to enhanced repopulation. Further studies will be required to determine the specific contribution of different renal cell fractions to recellularize kidney scaffolds, particularly those from different fetal and postnatal age groups.

Similar to the human fetus, the nephrogenic zone persists in the fetal rhesus monkey kidney until the third trimester. The cells that infiltrated the scaffolds stained positive for Pax2, which we have previously shown are restricted to the nephrogenic zone during the early third trimester and localized to the cortical collecting ducts and inner medullary regions of the renal papilla.[17] Although additional analysis would be required, findings by others[37] suggest a renal progenitor population may exist in the renal papilla that may be Pax2+. The tubules found within recellularized scaffolds also expressed calbindin, which has been shown in the ureteric bud and in the collecting ducts during the third trimester and in the postnatal kidney. Markers of mesenchyme (vimentin), epithelium (cytokeratin), and endothelium (CD31), as well as SMA (expressed in metanephric mesenchyme and the glomerular tuft), provided a combination of markers used to characterize cells that infiltrated the scaffold and showed tubular branching. Additional studies will be necessary to more extensively explore the cells that repopulate renal ECM and their functional capabilities.

To enhance repopulation of the scaffolds, cytokine-enriched medium was also assessed. The addition of FGF to the culture medium enhanced formation of mature tubules with scaffold repopulation noted consisting of large clusters of vimentin+ cytokeratin+ cells. Although addition of high doses of FGF to cell culture has been reported to inhibit tubulogenesis, FGF is a strong inhibitor of apoptosis of tubular epithelial precursors, capillary precursors, and regulatory cells of the ureteric bud.[38,39] Because we used a low dose of FGF (4 ng/mL) the benefits of tubular epithelial cell rescue may have outweighed the inhibitory effects on tubulogenesis, resulting in enhanced repopulation. These results demonstrate the capacity of decellularized kidney sections to maintain tubules and serve as a framework for tubular growth. Moreover, formation of three-dimensional renal structures did not occur when dissociated cells were used. Intact tubules and renal structures provided the best environment in which to form tubules in the decellularized kidney scaffolds in these studies. Further investigations will be required to assess the functional properties of these engineered renal constructs.

Taken together, these data provide initial insights into the *in vitro* renal tissue engineering of decellularized kidney scaffolds, and address the impact of donor age and cellular approach on recellularization. These findings provide useful methods to explore tissue regeneration strategies for the potential future treatment of kidney disease, and in a variety of age groups.

Acknowledgments

The authors wish to thank Michele Martinez for assistance with qRT-PCR. These studies were supported by the NIH Center of Excellence in Translational Human Stem Cell Research (grant #HL085036), California Institute for Regenerative Medicine (CIRM) Comprehensive grant (#RC1-00144), the UC Davis Stem Cell Training Program (CIRM, #T1-00006 and TG2-01163), the CTSC T32 Pre-Doctoral Clinical Research Training Program (5TL1RR024145-02), and the CNPRC base operating grant (#RR00169).

Disclosure Statement

No competing financial interests exist.

References

1. National Kidney Foundation: Kidney disease. Available at www.kidney.org/kidneyDisease/ (accessed 7/18/2010).
2. U.S. Department of Health and Human Services. HRSA/OPTN. Available at http://optn.transplant.hrsa.gov/latestData/viewDataReports.asp (accessed 7/18/2010).
3. Ott, H.C., Matthiesen, T.S., Goh, S.K., Black, L.D., Kren, S.M., Netoff, T.I., and Taylor, D.A. Perfusion-decellularized matrix: using nature's platform to engineer a bioartificial heart. Nature **14,** 213, 2008.
4. Macchiarini, P., Jungebluth, P., Go, T., Asnaghi, M.A., Rees, L.E., Cogan, T.A., Dodson, A., Martorell, J., Bellini, S., Parnigotto, P.P., Dickinson, S.C., Hollander, A.P., Mantero, S., Conconi, M.T., and Birchall, M.A. Clinical transplantation of a tissue-engineered airway. Lancet **372,** 2023, 2008.
5. Conconi, M.T., De Coppi, P., Di Liddo, R., Vigolo, S., Zanon, G.F., Parnigotto, P.P., and Nussdorfer, G.G. Tracheal matrices, obtained by a detergent-enzymatic method, support *in vitro* the adhesion of chondrocytes and tracheal epithelial cells. Transpl Int **18,** 727, 2005.
6. Uygun, B.E., Soto-Gutierrez, A., Yagi, H., Izamis, M.L., Guzzardi, M.A., Shulman, C., Milwid, J., Kobayashi, N., Tilles, A., Berthiaume, F., Hertl, M., Nahmias, Y., Yarmush, M.L., and Uygun, K. Organ reengineering through development of a transplantable recellularized liver graft using decellularized liver matrix. Nat Med **7,** 814, 2010.
7. Petersen, T.H., Calle, E.A., Zhao, L., Lee, E.J., Gui, L., Raredon, M.B., Gavrilov, K., Yi, T., Zhuang, Z.W., Breuer, C., Herzog, E., and Niklason, L.E. Tissue-engineered lungs for *in vivo* implantation. Science **329,** 538, 2010.
8. Price, A.P., England, K.A., Matson, A.M., Blazar, B.R., and Panoskaltsis-Mortari, A. Development of a decellularized lung bioreactor system for bioengineering the lung: the matrix reloaded. Tissue Eng **16,** 2581, 2010.
9. Ott, H.C., Clippinger, B., Conrad, C., Schuetz, C., Pomerantseva, I., Ikonomou, L., Kotton, D., and Vacanti, J.P. Regeneration and orthotopic transplantation of a bioartificial lung. Nat Med **16,** 927, 2010.
10. Kanwar, Y.S., Wada, J., Lin, S., Danesh, F.R., Chugh, S.S., Yang, Q., Banerjee, T., and Lomasney, J.W. Update of extracellular matrix, its receptors, and cell adhesion molecules in mammalian nephrogenesis. Am J Renal Physiol **286,** F202, 2004.
11. Woolf, A.S., Palmer, S.J., Snow, M.L., and Fine, L.G. Creation of a functioning chimeric mammalian kidney. Kidney Int **38,** 991, 1990.
12. Nakayama, K.H., Batchelder, C.A., Lee, C.C., and Tarantal, A.F. Decellularized rhesus monkey kidney as a three-dimensional scaffold for renal tissue engineering. Tissue Eng **16,** 2207, 2010.
13. Jimenez, D.F., Lee, C.I., O'Shea, C.E., Kohn, D.B., and Tarantal, A.F. HIV-1-derived lentiviral vectors and fetal route of administration on transgene biodistribution and expression in rhesus monkeys. Gene Ther **12,** 821, 2005.
14. Leapley, A.C., Lee, C.C., Batchelder, C.A., Yoder, M.C., Matsell, D.G., and Tarantal, A.F. Characterization and culture of fetal rhesus monkey renal cortical cells. Pediatr Res **66,** 448, 2009.
15. Kreisberg, J.I., and Karnovsky, M.J. Glomerular cells in culture. Kidney Int **23,** 439, 1983.
16. Batchelder, C.A., Lee, C.C., Martinez, M.L., and Tarantal, A.F. Ontogeny of the kidney and renal developmental markers in the rhesus monkey (*Macaca mulatta*). Anat Rec **29,** 1971, 2010.
17. Batchelder, C.A., Lee, C.C., Matsell, D.G., Yoder, M.C., and Tarantal, A.F. Renal ontogeny in the rhesus monkey (*Macaca mulatta*) and directed differentiation of human embryonic stem cells towards kidney precursors. Differentiation **78,** 45, 2009.
18. Chen, J., Boyle, S., Zhao, M., Su, W., Takahashi, K., Davis, L., Decaestecker, M., Takahashi, T., Breyer, M.D., and Hao, C.M. Differential expression of the intermediate filament protein nestin during renal development and its localization in adult podocytes. J Am Soc Nephrol **17,** 1283, 2006.
19. el-Kassaby, A., AbouShwareb, T., and Atala, A. Randomized comparative study between buccal mucosal and acellular bladder matrix grafts in complex anterior urethral strictures. J Urol **179,** 1432, 2008.
20. Saxen, L. Organogenesis of the Kidney. Cambridge: Cambridge University Press, 1987.
21. Ross, E.A., Williams, M.J., Hamazaki, T., Terada, N., Clapp, W.L., Adin, C., Ellison, G.W., Jorgensen, M., and Batich, C.D. Embryonic stem cells proliferate and differentiate when seeded into kidney scaffolds. J Am Soc Nephrol **20,** 2338, 2009.
22. Hopkins, C., Li, J., Rae, F., and Little, M.H. Stem cell options for kidney disease. J Pathol **217,** 265, 2009.
23. Zhang, Y., He, Y., Bharadwaj, S., Hammam, N., Carnagey, K., Myers, R., Atala, A., and Van Dyke, M. Tissue-specific extracellular matrix coatings for the promotion of cell proliferation and maintenance of cell phenotype. Biomaterials **30,** 4021, 2009.
24. Tottey, S., Johnson, S.A., Crapo, P.M., Reing, J.E., Zhang, L., Jiang, H., Medberry, C.J., Reines, B., and Badylak, S.F. The effect of source animal age upon extracellular matrix scaffold properties. Biomaterials **32,** 128, 2011.
25. Hacia, J.G., Lee, C.C.I., Jimenez, D.F., Karaman, M.W., Ho, V.V., Siegmund, K.D., and Tarantal, A.F. Age-related gene expression profiles of rhesus monkey bone marrow-derived mesenchymal stem cells. J Cell Biochem **103,** 1198, 2008.
26. Lee, C.C., Ye, F., and Tarantal, A.F. Comparison of growth and differentiation of fetal and adult rhesus monkey mesenchymal stem cells. Stem Cells Dev **15,** 209, 2006.
27. Lee, C.C.I., Fletcher, M.D., and Tarantal, A.F. Effect of age on the frequency, cell cycle, and lineage maturation of rhesus monkey (*Macaca mulatta*) $CD34^+$ and hematopoietic progenitor cells. Pediatr Res **58,** 315, 2005.
28. Shelley, W.C., Leapley, A.C., Huang, L., Critser, P.J., Mead, L.E., Zeng, P., Prater, D., Ingram, D.A., Tarantal, A.F., and Yoder, M.C. Changes in the frequency and *in vivo* vessel forming ability of rhesus monkey circulating endothelial colony forming cells (ECFC) across the lifespan (Birth to aged). Pediatr Res (In press).

29. Dekel, B., Burakova, T., Arditti, F.D., Reich-Zeliger, S., Milstein, O., Aviel-Ronen, S., Rechavi, G., Friedman, N., Kaminski, N., Passwell, J.H., and Reisner, Y. Human and porcine early kidney precursors as a new source for transplantation. Nat Med **9,** 53, 2003.
30. Kim, S.S., Gwak, S.J., Han, J., Park, H.J., Park, M.H., Song, K.W., Cho, S.W., Rhee, Y.H., Chung, H.M., and Kim, B.S. Kidney tissue reconstruction by fetal kidney cell transplantation: effect of gestation stage of fetal kidney cells. Stem Cells **25,** 1393, 2007.
31. Jorau, A., Stern, K.A., Atala, A., and Yoo, J.J. *In vitro* generation of three-dimensional renal structures. Methods **47,** 129, 2009.
32. Humphreys, B.D., Valerius, M.T., Kobayashi, A., Mugford, J.W., Soeung, S., Duffield, J.S., McMahon, A.P., and Bonventre, J.V. Intrinsic epithelial cells repair the kidney after injury. Cell Stem Cell **2,** 284, 2008.
33. Humphreys, B.D., Czerniak, S., DiRocco, D.P., Hasnain, W., Cheema, R., and Bonventre, J.V. Repair of injured proximal tubule does not involve specialized progenitors. Proc Natl Acad Sci U S A **108,** 9226, 2011.
34. Little, M.H., and Bertram, J.F. Is there such a thing as a renal stem cell? J Am Soc Nephrol **20,** 2112, 2009.
35. Ivanova, L., Hiatt, M.J., Yoder, M.C., Tarantal, A.F., and Matsell, D.G. Ontogeny of CD24 in the human kidney. Kidney Int **77,** 1123, 2010.
36. Ronconi, E., Sagrinati, C., Angelotti, M.L., Lazzer, E., Mazzinghi, B., Ballerini, L., Parente, E., Becherucci, F., Gacci, M., Carini, M., Maggi, E., Serio, M., Vannelli, G.B., Lasagni, L., Romagnani, S., and Romagnani, P. Regeneration of glomerular podocytes by human renal progenitors. J Am Soc Nephrol **20,** 322, 2009.
37. Al-Awqati, Q., and Oliver, J.A. The kidney papilla is a stem cell niche. Stem Cell Rev **2,** 181, 2006.
38. Dudley, A.T., Godin, R.E., and Robertson, E.J. Interaction between FGF and BMP signaling pathways regulated development of metanephric mesenchyme. Genes Dev **13,** 1601, 1999.
39. Barasch, J., Qiao, J., McWilliams, G., Chen, D., Oliver, J.A., and Herzlinger, D. Ureteric bud cells secrete multiple factors, including bFGF, which rescue renal progenitors from apoptosis. Am J Physiol Renal Physiol **273,** 757, 1997.

Address correspondence to:
Alice F. Tarantal, Ph.D.
Center of Excellence in Translational Human Stem Cell Research
California National Primate Research Center
University of California
Pedrick and Hutchison Roads
Davis, CA 95616-8542

E-mail: aftarantal@primate.ucdavis.edu

Received: December 11, 2010
Accepted: July 7, 2011
Online Publication Date: October 5, 2011